Biomacromolecules

pubs.acs.org/Biomac

Article

Protein Vesicles Self-Assembled from Functional Globular Proteins with Different Charge and Size

Dylan R. Dautel and Julie A. Champion*

Cite This: *Biomacromolecules* 2021, 22, 116–125

Read Online

ACCESS | Metrics & More | Article Recommendations | Supporting Information

ABSTRACT: Protein vesicles can be synthesized by mixing two fusion proteins: an elastin-like polypeptide (ELP) fused to an arginine-rich leucine zipper (Z_R) with a globular, soluble protein fused to a glutamate-rich leucine zipper (Z_E). Currently, only fluorescent proteins have been incorporated into vesicles; however, for protein vesicles to be useful for biocatalysis, drug delivery, or biosensing, vesicles must assemble from functional proteins that span an array of properties and functionalities. In this work, the globular protein was systematically changed to determine the effects of the surface charge and size on the self-assembly of protein vesicles. The formation of microphases, which included vesicles, coacervates, and hybrid structures, was monitored at different assembly conditions to determine the phase space for each globular protein. The results show that the protein surface charge has a small effect on vesicle self-assembly. However, increasing the size of the globular protein decreases the vesicle size and increases the stability at lower Z_E/Z_R molar ratios. The phase diagrams created can be used as guidelines to incorporate new functional proteins into vesicles. Furthermore, this work reports catalytically active enzyme vesicles, demonstrating the potential for the application of vesicles as biocatalysts or biosensors.

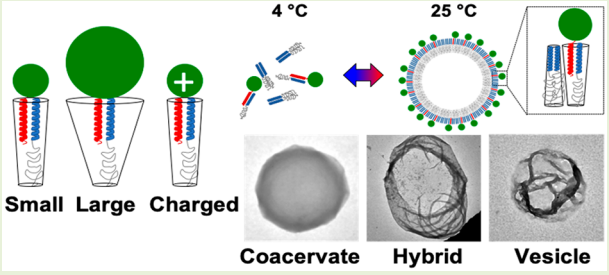

INTRODUCTION

Vesicles are hollow membranous structures composed of amphiphiles. Their unique ability to encapsulate small molecules or enzymes allows for a controlled, protective environment surrounding these molecules and has led to interest in developing vesicles for drug delivery applications[1,2] and use as microreactors,[3,4] biosensors,[5] and artificial organelles.[6] Synthetic vesicles are typically constructed from lipids (liposomes) or polymers (polymersomes). Additionally, vesicles have been synthesized from globular protein−polymer conjugates called proteinosomes.[7] However, methods to synthesize vesicles solely from recombinant proteins have recently been developed.[8−10] Vesicles assembled directly from proteins have several advantages, including tunability through genetic modification and the ability to incorporate functional, folded proteins onto the vesicle surface without additional processing steps that can lead to protein denaturation and loss of function.[4,11]

Our group has reported the self-assembly of vesicles from two recombinant fusion proteins, Z_R-ELP (elastin-like polypeptide) and globule-Z_E, in aqueous solutions above a critical salt concentration.[9] One particular advantage of these vesicles is the hydrophilic domain, globule-Z_E, which contains a globular, functional protein capable of endowing vesicles with biocatalytic or binding properties. The globular protein is genetically fused to a glutamate-rich leucine zipper (Z_E) that has picomolar affinity for its arginine-rich leucine zipper (Z_R) binding partner. The leucine zipper pair connects the hydrophilic globule-Z_E domain to the hydrophobic domain, Z_R-ELP, creating an amphiphilic complex. ELPs are derived from the human protein tropoelastin and undergo hydrophobic conformational changes when heated, resulting in lower critical solution temperature (LCST) behavior.[12,13] The LCST behavior of ELPs drive vesicle formation through a transient coacervate phase when mixtures of globule-Z_E and Z_R-ELP are heated from 4 °C to room temperature in aqueous solutions (Figure 1a).[14] In addition to the heterodimeric Z_E/Z_R leucine zipper pair, the vesicles also contain Z_R homodimers, which have ~10^{-6} M affinity.[15] The design of the fusion proteins allows for the direct incorporation of functional globular proteins into vesicles at a defined (<1) molar ratio of globule-Z_E to Z_R-ELP (Z_E/Z_R). Vesicle properties have been shown to be dependent on Z_E/Z_R ratio, protein concentration, salt concentration, formation temperature, and globule-Z_E.[9,10]

The assembly of vesicles can be predicted based on the amphiphile packing, which is governed by a dimensionless molecular packing parameter, $P = V/(a_0 l_c)$.[22,23] Due to thermodynamic and geometric constraints, vesicle formation

Special Issue: Bioinspired Macromolecular Materials

Received: April 29, 2020
Revised: July 10, 2020
Published: September 4, 2020

https://dx.doi.org/10.1021/acs.biomac.0c00671
Biomacromolecules 2021, 22, 116–125

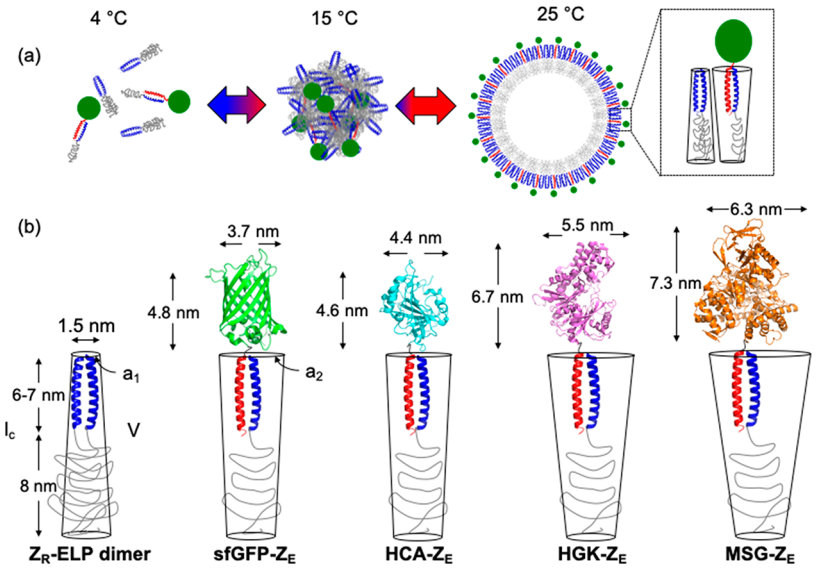

Figure 1. Schematics of the vesicle assembly and protein building blocks. (a) The transition from soluble protein to vesicles through a transient coacervate phase. The globular protein is shown as a green circle, ELP in gray, Z_E is red, and Z_R in blue.[16] (b) Approximate packing dimensions of Z_R-ELP, sfGFP-Z_E (green, PDB: 2B3P),[17] HCA-Z_E (cyan, PDB: 1CAY),[18] HGK-Z_E (magenta, PDB: 1 V4S),[19] and MSG-Z_E (orange, PDB 1D8C)[20] into vesicles.[21]

is expected when $1/2 < P < 1$. The packing parameter depends on the volume of the hydrophobic block (V), the average area of the hydrophobic interface that is shielded from interacting with water by the hydrophilic block (a_0), and the length of the hydrophobic tail (l_c). In this work, a_0 was taken as the weighted average of the interfacial area shielded by the rod-shaped Z_R homodimers (a_1) and the globule-Z_E domain (a_2) (Figure 1b).

Hydrophilic group charge and size are important parameters that affect amphiphile packing. Theoretically, increasing the charge of the hydrophilic group decreases the P value of amphiphilic molecules because it increases the electrostatic repulsion between hydrophilic blocks, resulting in an increased a_0 value.[22,24] Decreases in the packing parameter lead to increased curvature and smaller vesicles. Molecular charge also has other roles in the assembly of supramolecular structures. Olsen et al. showed that decreasing the net charge of green fluorescent protein (GFP) covalently bound to poly(*N*-isopropylacrylamide) (PNIPAM), a thermoresponsive synthetic polymer similar to ELP, enhanced the assembly in bulk polymer solutions because the decrease in the electrostatic repulsion increased the aggregation of the polymer.[25] Liu et al. also demonstrated that supercharging proteins decreases protein aggregation and hydrophobic interactions.[26] Similar to charge, increasing the hydrophilic group size results in repulsion between the hydrophilic blocks due to steric constraints, increasing a_0 and reducing the size of supramolecular structures. Additionally, polymersomes made from polymers with larger hydrophilic volume fractions increase the stability and decrease the permeability and fluidity of the polymersome.[27]

Here, we investigate the effects of altering the charge and size of globule-Z_E on vesicle self-assembly to develop design guidelines for the incorporation of new globular domains into recombinant protein vesicles. To alter the charge of globule-Z_E, three charged variants of superfolder green fluorescent protein (sfGFP) were designed with net surface charges of −10, 0, and +10. Three monomeric enzymes, human carbonic anhydrase II (HCA), human glucokinase (HGK), and *E. coli* malate synthase G (MSG), with molecular weights of 30 kDa, 50 kDa, and 80 kDa, respectively, were used to determine the effects of globule-Z_E size on vesicle self-assembly. The phase space of vesicle self-assembly was investigated for each protein. The results of this study enabled the development of a rational approach to select proteins that can be incorporated into protein vesicles and also revealed strategies to tune the vesicle size and morphology. Since vesicles are assembled from active enzymes, this work also demonstrates the potential of protein vesicles for biocatalysis or biosensing applications.

EXPERIMENTAL SECTION

Expression and Purification of Fusion Proteins. The pET28a-sfGFP-Z_E-His plasmids with sfGFP variants were purchased from Genscript. Plasmids pET28a-HCA-Z_E-His, pET28a-HGK-Z_E-His, and pET28a-MSG-Z_E-His were purchased from Twist Biosciences. The sfGFP-Z_E variants, MSG-Z_E, and HCA-Z_E were expressed in *Escherichia coli* strain BL21(DE3) star. To express these proteins, 1 L of lysogeny broth (LB) containing 50 mg of kanamycin was inoculated with 5 mL of overnight culture at 37 °C, and expression was induced once the culture reached an optical density at 600 nm (OD600) of 0.6−0.8 with 1.0 mM isopropyl β-D-1 thiogalactopyranoside (IPTG). Then, 5 h after induction, the cultures were harvested by centrifugation at 4000 *g* for 10 min. The pellets were then resuspended in lysis buffer containing 300 mM NaCl, 50 mM NaH_2PO_4, and 10 mM imidazole and lysed by sonication. After centrifugation at 10000 relative centrifugal force (rcf) for 30 min, the supernatant was incubated with Ni-nitrilotriacetic acid (NTA) agarose resin (Qiagen) for 1 h at 4 °C. The suspension was flowed through an Econo-Column (Biorad) and washed with 100 mL of 25 mM imidazole for MSG-Z_E and sfGFP-Z_E variants or 50 mM imidazole for HCA-Z_E, and ten 1 mL elutions were collected using 250 mM imidazole. After verifying the purity by sodium dodecyl sulfate polyacrylamide gel electrophoresis (SDS-PAGE), the purified proteins were buffer exchanged into phosphate buffered saline (PBS) by dialysis with three buffer exchanges at 4 °C, including an overnight incubation.

HGK-Z_E was expressed the same as HGK was previously.[28,29] Briefly, pET28a-HGK-Z_E-His was transformed into *E. coli* strain BL21(DE3) pLysS and grown by inoculating 5 mL of overnight

https://dx.doi.org/10.1021/acs.biomac.0c00671
Biomacromolecules 2021, 22, 116−125

culture into 1 L of LB containing 50 mg of kanamycin and 34 mg of chloramphenicol at 37 °C and allowing the culture to grow to OD600 of 0.6. The temperature of the culture was then reduced to 22 °C and induced with 0.4 mM IPTG. Cells were harvested 5 h later by centrifugation at 4000 *g* for 10 min. HGK-Z_E was then purified using affinity chromatography as described for MSG-Z_E. After collecting elutions, the enzyme was buffer exchanged into phosphate-buffered saline (PBS) with 1 mM DTT. HGK-Z_E was then further purified by size exclusion chromatography (GE AKTA pure 25 FPLC) with a GE HiPrep Sephacryl S-100 HR column for a final yield of ∼0.2 mg/L of culture.

The gene for Z_R-ELP, contained in pQE60-His-Z_E/Z_R-ELP, a kind gift from Prof. David Tirrell, was coexpressed with His-Z_E in AF-IQ BL21(DE3) *E. coli* in 1 L of LB containing 200 mg of ampicillin and 34 mg of chloramphenicol and harvested by centrifugation at 4000 rcf for 10 min.[30] Z_R-ELP was also purified by affinity chromatography with the same resin and columns as above. Cells were lysed using denaturing conditions in 8 M urea, 100 mM NaH_2PO_4, and 10 mM TrisCl at pH 8.0; washed with 8 M urea buffer at pH 6.3; and eluted using 6 M guanidine hydrochloride, 100 mM NaH_2PO_4, and 10 mM TrisCl, as in our past work.[9,10,14] Z_R-ELP was then buffer exchanged into mQ water over 2 days with extensive buffer changes, freeze-dried for long-term storage, and dissolved in cold mQ water for use. SDS-PAGE was used to verify the purity of all proteins. Amino acid and DNA sequences are available in the Supporting Information.

Measuring Transition Temperature. To measure the transition temperature (T_t) of the globule-Z_E and Z_R-ELP complexes, the turbidity of solutions containing 30 μM Z_R-ELP and 1.5 μM globule-Z_E was measured every minute as the temperature increased at a ramp rate of 1 °C/min from 5 to 40 °C by measuring the optical density at 400 nm (Chirascan-plus CD, Applied Photophysics). T_t was determined by finding the inflection point.

Characterization Techniques for Vesicles and Other Structures. All solutions were prepared on ice in Greiner round-bottom 96-well plates by adding mQ water, Z_R-ELP, globule-Z_E, and a 10× PBS solution at the specified concentrations. The 10× PBS solution contains 1.4 M NaCl, 100 mM Na_2HPO_4, 27 mM KCl, and 18 mM KH_2PO_4. All salt concentrations are reported with respect to the NaCl concentration. The turbidity of each solution was obtained by measuring the absorbance of the solution at 400 nm with a Biotek Instrument Synergy H4 Hybrid multimode microplate reader as the solution was heated to 25 °C for 60 min. To determine the size of structures that formed, dynamic light scattering (DLS) (Malvern Instruments Zetasizer NanoZS) was performed using the intensity mode with a 4 mW He−Ne laser with a wavelength of 633 nm to detect backscattering (173°). The *Z*-average was used to report the size of vesicles except in the case when multiple peaks were present; in this case the peak size was used. DLS measurements were determined to be quality readings if they met two criteria.[31] First, the particles had to meet the quality standards of the instrument, and upon a visual inspection of the correlogram, the particles had low polydispersity and did not settle or aggregate.

Imaging for sfGFP-Z_E vesicles was performed with a Zeiss LSM 700 confocal microscope using a 63× immersion lens. HCA-Z_E, HGK-Z_E, and MSG-Z_E were labeled with Alexa Fluor 488 succinimidyl ester (AF488) by incubating 2 μg of AF488 with 0.4 mg of protein in a sodium carbonate buffer (pH 8.0) for 1 h followed by immediate buffer exchanges to remove unreacted dye. Structures containing the proteins were imaged by epifluorescent microscopy (Zeiss Axio Observer Z1) with a 100× immersion lens or confocal microscopy. Transmission electron microscopy (JE0L 100 CXII) operated at 100 kV was used to obtain higher resolution images of smaller vesicles and hybrid structures. Transmission electron microscopy (TEM) grids were prepped by dispensing 10 μL of sample on copper grids (Electron Microscopy Sciences) and letting the sample adhere for 10 min. Then, the grids were washed with 10 μL of mQ water, negatively stained with 10 μL of 1% phosphotungstic acid, and washed again with 10 μL of mQ water for 10−20 s each. After each step, the liquid was blotted from the grid using filter paper. Before imaging, the grid was covered and left to dry overnight.

Enzymatic Activity Assays. Activity assays were conducted by adding equal masses of either soluble enzyme or enzyme that had been incorporated into vesicles to the assay solution. The assays were performed in 200 μL solutions that contained 0.5 M PBS at a pH of 7.4 and 30 °C to ensure vesicle stability. The absorbance for all activity assays were measured using a Biotek Instrument Synergy H4 Hybrid multimode microplate reader, and the absorbance was related to the enzymatic activity using Beer's law. All assay components were purchased from Millipore Sigma.

HCA-Z_E activity was measured by adding 10 μg of HCA-Z_E to solutions containing 10 mM $ZnSO_4$ and 1 mM 4-nitrophenyl acetate and monitoring the absorbance of the solution at a wavelength of 348 nm. The absorbance of the solution was related to the concentration of product, 4-nitrophenol, using Beer's law. The extinction coefficient of 4-nitrophenol used was 5400 M^{-1} cm^{-1}.[32]

A coupled enzyme assay was used to measure the HGK-Z_E activity by adding 1 μg of HGK-Z_E to solutions of 5 mM $MgCl_2$, 1 mM ATP, 50 mM glucose, 2 units of glucose-6-phosphate dehydrogenase from *Saccharomyces cerevisiae*, 0.5 mM NADPH, and 1 mM DTT to prevent the formation of disulfide bonds between free cysteine residues. First, HGK converts glucose to glucose-6-phosphate in the presence of ATP and Mg^{2+}, which is then consumed by glucose-6-phosphate dehydrogenase in the presence of NADPH.[19] The change in concentration of NADPH was quantified by measuring the change in the absorbance of the solution at 340 nm using an extinction coefficient of 6220 M^{-1} cm^{-1}.

To determine the activity of MSG-Z_E, 0.25 μg of MSG-Z_E was added to solutions containing 1 mM glyoxylate, 5 mM $MgCl_2$, 0.25 mM Acetyl CoA, and the absorbance of the solution at 232 nm was measured in UV transparent Corning CoStar 96 well plates.[20] The loss of the absorbance of the solution at 232 nm is related to the consumption of acetyl CoA. The extinction coefficient of acetyl CoA, 4500 M^{-1} cm^{-1}, was used to determine the change in concentration of acetyl CoA.

RESULTS AND DISCUSSION

Effects of Globule-Z_E Charge on Vesicle Self-Assembly. In general, the surfaces of globular proteins are composed of a combination of polar, charged, and hydrophobic amino acids that shield buried hydrophobic residues. This is considerably different than the hydrophilic headgroups of liposomes or the hydrophilic blocks of polymersomes, which are made up of single small molecules or repeating units, respectively. Since proteins contain many charged residues, the net charge of proteins can be in excess of ±30 but is more commonly between ±10.[33] To determine the effects of charge on vesicle self-assembly, three monomeric variants of superfolder green fluorescent protein-Z_E were designed: sfGFP-Z_E(−10), sfGFP-Z_E(0), and sfGFP-Z_E(+10), with net surface charges of −10, 0, and +10, respectively. Changes to the tertiary structure of the sfGFP-Z_E variants were limited by altering the most highly solvent exposed charged or polar residues using the Rosetta online supercharging platform, and when possible, glutamine residues were mutated to glutamic acid and asparagine to aspartic acid.[26,34] Since ELP can be sensitive to pH changes and the molecular packing is altered by changing the globular protein, varying the charge of the globular protein allows for the isolation of charge as the only variable impacting supramolecular assembly.[35] SDS-PAGE and zeta potential were used to demonstrate that each variant had different surface charges (Figure S1 and Table S1).

Salt concentration plays a key role in the self-assembly of protein vesicles because ELPs are responsive to ionic strength. The minimum salt concentration to form stable vesicles was 0.9 M PBS for all three charged variants in solutions containing 30 μM Z_R-ELP and 0.05 Z_E/Z_R. Also, the transition

https://dx.doi.org/10.1021/acs.biomac.0c00671
Biomacromolecules 2021, 22, 116−125

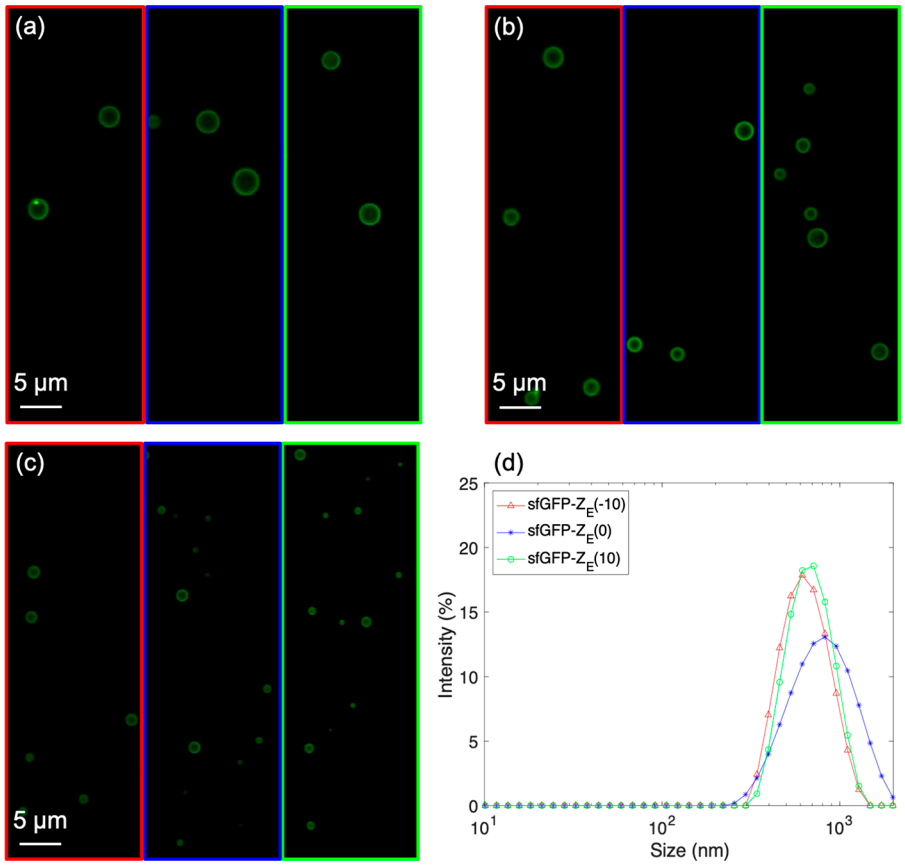

Figure 2. Effect of increasing the charged variant on vesicle self-assembly. sfGFP-$Z_E(-10)$, sfGFP-$Z_E(0)$, and sfGFP-$Z_E(+10)$ vesicles are shown in red, blue, and green boxes, respectively. Vesicles were formed in solutions containing 1.0 M PBS with a Z_E/Z_R ratio of (a) 0.01, (b) 0.05, and (c) 0.10. (d) Size intensity plot of vesicles formed in 1.0 M PBS, 0.10 Z_E/Z_R, 30 μM Z_R-ELP.

temperature for each was identical (Figure S2). These results indicated that the charge of the globular protein did not impact the strong effect of salt on ELP. Typically, increasing the salt concentration decreases T_t and increases the ELP hydrophobicity.[36] Additionally, with increasing ionic strength, ELPs become folded into tightly packed structures, decreasing V.[37,38] Altogether, these effects reduced the packing parameter below 1 and supported vesicle formation from coacervate above a minimum salt concentration. Increasing the salt concentration further above the minimum salt concentration to 1.5 M PBS led to decreased vesicle size for all three sfGFP-Z_E variants (Figure S3). This is different from the behavior of liposomes, which increase in size when the ionic strength of NaCl is increased from 10 to 400 mM due to the effects of charge screening.[39]

Next, to determine if an increased charged content affected vesicle self-assembly, the amount of sfGFP-Z_E incorporated into vesicles was changed by varying the Z_E/Z_R ratio from 0.01 to 0.10. Increasing the Z_E/Z_R ratio decreased the size of the vesicles (Figure 2a–c). However, there was no difference in the size between the sfGFP-Z_E variants for a given Z_E/Z_R ratio, suggesting that the increased area (a_0) of the hydrophilic group for larger ratios was responsible for increasing the curvature and not the electrostatic repulsion (Figure 2d). The electrostatic repulsion between globular proteins should contribute positively to the free energy of formation, destabilizing the supramolecular assembly and leading to the formation of structures with larger a_0 values, such as smaller vesicles, cylindrical micelles, or micelles.[40] However, the Debye length, which is a measure of how far a molecule's electrostatic effect persists, is inversely proportional to the ionic strength of the solution.[22] The dampening of electrostatic effects at high salt concentrations, or charge screening, was likely responsible for the similar size of vesicles assembled from the sfGFP-Z_E variants because, at above 0.3 M ionic strength, ions shield the electrostatic effects between globule-Z_E domains.[39] Since the minimum salt concentration for vesicle formation is 0.9 M at room temperature, charge plays a small role in vesicle self-assembly.

Altogether, these results show that protein vesicle self-assembly is relatively robust with respect to globular protein charge and can be tuned, as needed, for different applications. For example, charge plays an important role in biodistribution and the interactions of enzyme substrates with surfaces.[41,42] While not affected by charge, the observation that increasing the Z_E/Z_R ratio decreased vesicle size demonstrates the role of steric repulsion between globular proteins in vesicle self-assembly and predicts that globule-Z_E size will have a significant effect on vesicles.

Effects of Globule-Z_E Size on Vesicle Self-Assembly. The globular monomeric enzymes HCA, HGK, and MSG with molecular weights of 30, 50, and 80 kDa were chosen to determine the effects of protein size on vesicle self-assembly and enable the quantitative assessment of globular protein activity in vesicles. The phase space of globule-Z_E/Z_R-ELP complexes was probed by varying the salt concentration, Z_R-ELP concentration, and Z_E/Z_R ratio for each enzyme. Varying the Z_E/Z_R ratios and ionic strength of each globular enzyme

https://dx.doi.org/10.1021/acs.biomac.0c00671
Biomacromolecules 2021, 22, 116–125

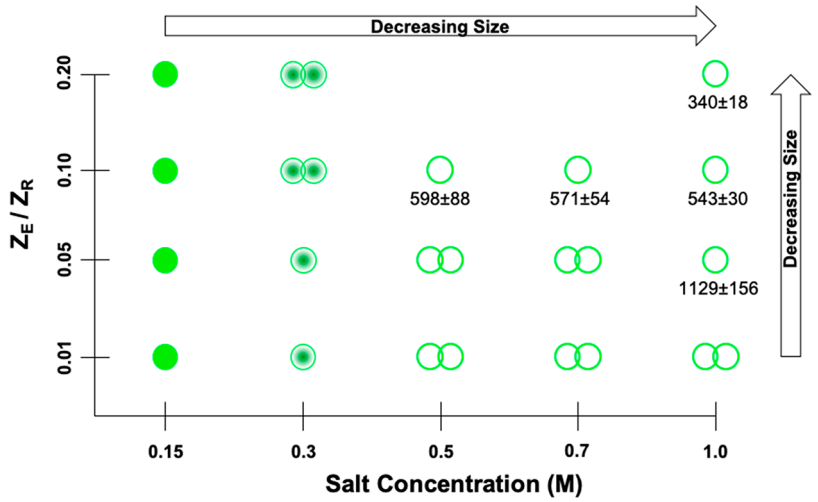

Figure 3. Phase space of mixtures of 10 μM Z_R-ELP and HCA-Z_E at 25 °C. Filled circles represent the formation of coacervates. Partially filled circles represent the formation of hybrid structures. Two fused circles represent the formation of fused structures (vesicles or vesicle−coacervate hybrids). Hollow circles represent the formation of stable vesicles. The hydrodynamic diameters and standard deviations of vesicles in units of nm are listed underneath stable structures.

over a range of conditions allowed us to observe consistent trends between the size of the globule-Z_E domain and the self-assembly of vesicles. Previous work showed that dimeric interactions between enhanced GFP impacted the a_0 values and vesicle size.[9] In this work, only monomeric enzymes were incorporated into vesicles, as it may be difficult to deconvolute the effects of globular protein oligomerization on packing.

The phase space of mixtures of Z_R-ELP and HCA-Z_E was defined to determine if vesicles could self-assemble from small monomeric enzymes. Human carbonic anhydrase II is a 30 kDa cytosolic protein that catalyzes the simple yet critical physiological reaction of CO_2 to bicarbonate. In addition to their physiological importance, carbonic anhydrases have also drawn attention for carbon capture applications.[43] The phase space of globular domains containing HCA was probed by varying the Z_E/Z_R ratios from 0.01 to 0.20 and salt concentration from 0.15 to 1.0 M (Figure 3).

Five different structures were observed in this parameter space (Figure 4). At 0.15 M PBS, the only structures observed were protein-rich coacervate droplets (Figure S4). Increasing the salt concentration to 0.3 M PBS led to the formation of coacervate-vesicle hybrid and fused coacervate-vesicle hybrid structures. For these structures, fluorescent microscopy revealed the presence of a protein-rich ring on the exterior, indicative of vesicles, and also a protein dense interior similar to that of coacervates (Figure 4**a,c** and Figure S4). The turbidity profiles of these structures indicated that they were not stable colloidal structures, and their size could not be determined by DLS (Figure S5). The formation of hybrid structures was observed when the T_t of the solution was near the solution temperature (25 °C) and so not all the ELP had completed the transition based on the definition of the T_t at the point of greatest slope. The T_t of the HCA-Z_E/Z_R-ELP complexes at 0.3 M PBS was 27 °C (Figure S6). Epifluorescent microscopy and TEM images revealed the formation of vesicles from HCA-Z_E at salt concentrations of 0.5 M and higher (Figure 4**b,d** and Figure S7). However, at high salt concentrations and low Z_E/Z_R ratios, vesicles were not stable and aggregated together (Figure 4d). Increasing the Z_E/Z_R ratio decreased the aggregation of the vesicles and led to the formation of stable vesicles. As the salt concentration and the Z_E/Z_R ratio increased, turbidity profiles flattened signaling the formation of stable vesicles and the hydrodynamic diameter decreased according to DLS (Figure 3 and Figure S5), consistent with sfGFP vesicles.

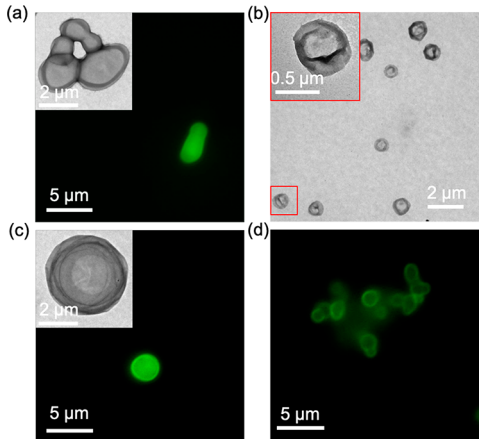

Figure 4. Confocal and TEM micrographs of phase structures that formed from mixtures of 10 μM Z_R-ELP and HCA-Z_E. (a) Fused hybrid coacervate-vesicle structures formed with 0.10 Z_E/Z_R and 0.3 M PBS. (b) Vesicles formed at 0.10 Z_E/Z_R and 1.0 M PBS. (c) Hybrid coacervate-vesicle structures formed with 0.05 Z_E/Z_R and 0.3 M PBS (d) Fused vesicles formed in 0.01 Z_E/Z_R and 1.0 M PBS.

As the ELP concentration in a solution increases, T_t decreases.[10,44] To determine if Z_R-ELP concentration played a role in the self-assembly of vesicles made from HCA-Z_E, the Z_R-ELP concentration was increased from 10 μM to 30 μM, and the phase space was probed (Figure S8−S10). Under some of the conditions that were probed, increasing the Z_R-ELP concentration reduced the salt concentration that was necessary to form stable vesicles due to lower T_t of the ELP. Vesicles formed in solutions of more concentrated Z_R-ELP also decreased in size at high salt and high Z_E/Z_R ratio but increased in size at moderate salt and moderate Z_E/Z_R ratios.

To determine if vesicles could self-assemble from large monomeric enzymes, the phase space of mixtures of MSG-Z_E,

https://dx.doi.org/10.1021/acs.biomac.0c00671
Biomacromolecules 2021, 22, 116−125

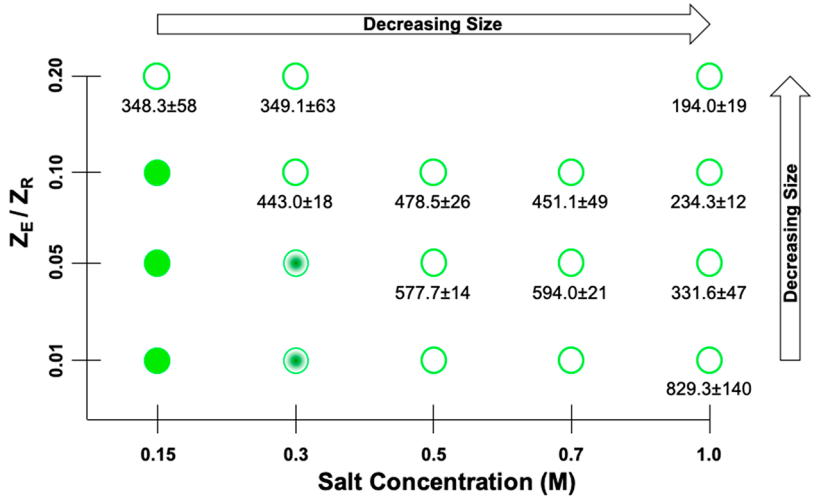

Figure 5. Phase space of mixtures of 10 μM Z_R-ELP and MSG-Z_E at 25 °C. Filled circles represent the formation of coacervates. Partially filled circles represent the formation of hybrid structures. Hollow circles represent the formation of stable vesicles. The hydrodynamic diameters and standard deviations of vesicles in nanometers are listed underneath stable structures.

an 80 kDa globular enzyme, and Z_R-ELP was determined. E. *coli* MSG is a Mg^{2+} dependent enzyme that converts glyoxylic acid to malic acid in the presence of acetyl CoA as part of the glyoxylate cycle.[20] Identical phase space conditions were used for HCA-Z_E and MSG-Z_E to compare the effects of globule-Z_E size on vesicle self-assembly (Figure 5).

Three distinct structures were observed from MSG-Z_E at 25 °C with confocal microscopy and TEM (Figure 6 and Figure S11). In solutions containing 0.15 M PBS and below 0.20 Z_E/Z_R, coacervates formed and sedimented, which led to decreased turbidity (Figure 6a and Figure S12). At 0.3 M PBS and Z_E/Z_R ratios below 0.10, hybrid structures were observed (Figure 6b). These hybrid structures were identified by TEM because they had the wrinkled structure of vesicles, and protein was present on the interior of the structures. In confocal micrographs, there was also the presence of a ring on the outer portion of the structures and a protein-rich phase on the interior (Figure 6b and Figure S12). This behavior was only observed at 0.3 M PBS, when the T_t of the MSG-Z_E–Z_R-ELP complex was 27 °C (Figure S6). Salt concentrations greater than 0.5 M PBS always led to the formation of vesicles, and increasing the Z_E/Z_R ratio led to an increased likelihood of observing vesicle formation with reliable DLS results (Figure 5 and Figure 6c). The effect of increasing the Z_R-ELP concentration from 10 to 30 μM was similar to what was observed for HCA-Z_E vesicles, where stable vesicle formation was observed at lower salt concentrations and lower Z_E/Z_R ratios (Figures S13–S15).

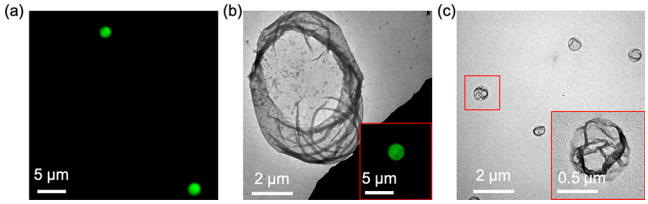

Figure 6. Confocal and TEM micrographs of phase structures that formed from mixtures of 10 μM Z_R-ELP and MSG-Z_E. (a) Coacervates observed in solutions containing 0.15 M PBS. (b) Coacervate–vesicle hybrid structures formed at 0.10 Z_E/Z_R and 0.3 M PBS. (c) Vesicles formed at 0.10 Z_E/Z_R and 1.0 M PBS.

To determine if supramolecular structures with more curvature could be formed from MSG-Z_E, such as micelles or cylindrical micelles, the Z_E/Z_R ratio was further increased from 0.20 to 0.40 and 0.80. Increasing the Z_E/Z_R ratio led to a reduction in the size of the vesicles from 348 nm at 0.20 Z_E/Z_R and 0.15 M PBS to 255 nm at 0.40 Z_E/Z_R. However, there was a saturation point, and at 0.80 Z_E/Z_R, a 13 nm peak was observed by DLS along with a vesicle peak near 255 nm (Figure S16). Since the Z_R-ELP concentration was kept constant and the MSG-Z_E concentration was increased, the peak is believed to be soluble MSG-Z_E.

There were two main differences between vesicles that self-assembled from HCA-Z_E and MSG-Z_E. First, HCA-Z_E vesicles showed more of a propensity to aggregate at lower Z_E/Z_R ratios. The HCA-Z_E vesicles were likely unstable at lower Z_E/Z_R ratios because HCA was not large enough to create an effective barrier between the hydrophobic ELP domain and the solution. Exposed ELP at the vesicle surface could have caused the vesicle aggregation and fusion. Second, in each condition that stable vesicles formed, the size of the MSG-Z_E vesicles were smaller (Figure 4 and Figure 6). This was expected, based on packing parameter theory, as the larger proteins had increased steric repulsions and formed structures with an increased curvature.

Although some differences exist, the vesicles assembled from both enzymes displayed similar trends. Vesicles formed from both enzymes decreased in size with an increasing salt concentration and Z_E/Z_R ratio just like vesicles assembled from sfGFP-Z_E variants. The HCA-Z_E/Z_R-ELP and MSG-Z_E/Z_R-ELP complexes also had the same transition temperature at 0.3 M PBS and exhibited similar phase transitions from coacervates to hybrid structures between 0.15 M PBS and 0.3 M PBS and from hybrid structures to vesicles between 0.3 M PBS and 0.5 M PBS (Figure 6 and Figure S7). These trends can be explained by the packing of amphiphiles into vesicles. Globular protein size affects the area that shields the hydrophobic surface from water, a_0. Increasing the size of the protein increased a_0 due to steric repulsions between proteins on the vesicle surface.[45] An increase in a_0 decreased

https://dx.doi.org/10.1021/acs.biomac.0c00671
Biomacromolecules 2021, 22, 116–125

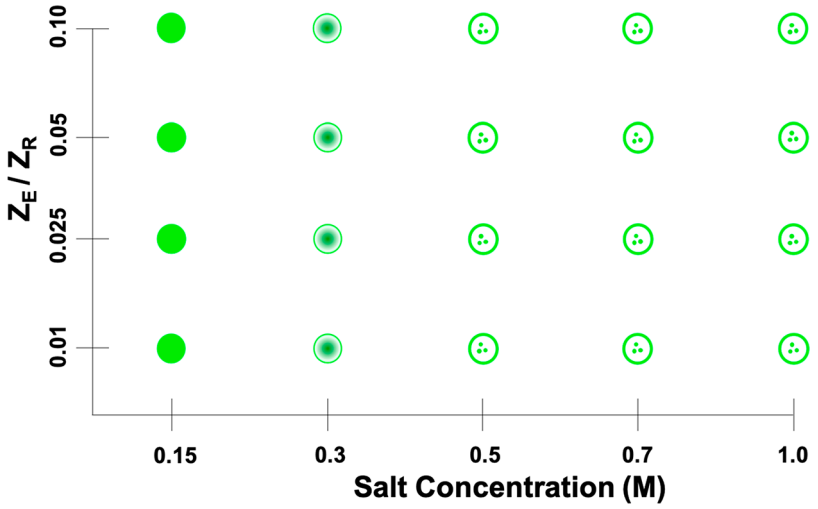

Figure 7. Phase space of mixtures of 10 μM Z_R-ELP and HGK-Z_E at 25 °C. Filled circles represent the formation of coacervates. Partially filled circles represent the formation of hybrid structures. Hollow circles with dots on the interior represent the formation of vesicles with entrapped coacervates.

the packing parameter ($P = V/(a_0 l_c)$), increasing the curvature and producing smaller vesicles. The size of proteins also impacts their hydrophobicity. Smaller proteins tend to be more hydrophobic because they are not bulky enough to bury hydrophobic residues, while larger proteins tend to be more hydrophilic.[46] Hydrophobic proteins are not likely to form vesicles because the protein complex formed by globule-Z_E and Z_R-ELP is not sufficiently amphiphilic. Additionally, larger more hydrophilic proteins should impact vesicle properties similarly to polymersomes with larger hydrophilic blocks, which typically exhibit increased stability and reduced permeability and fluidity of the polymersome.[47]

While molecular weight was the intended variable for this part of the work, each protein selected also had different primary sequences and structures. As such, it is not possible to only alter the molecular weight and hold all other protein physiochemical properties constant, as it would be for a polymer. This complication arose during the study of a medium-sized globular protein, human glucokinase (HGK), which is a 50 kDa enzyme that maintains glucose homeostasis by allosterically converting glucose to glucose-6-phosphate, signaling metabolic shifts in response to changing glucose concentrations. Unlike HCA and MSG, HGK contains four exposed, unpaired cysteines, which are capable of forming intermolecular disulfide bonds that can disrupt vesicle formation.[19] As before, salt concentrations and Z_E/Z_R ratios of solutions containing 10 μM Z_R-ELP were varied to construct the HGK-Z_E phase diagram (Figure 7).

In solutions containing 0.15 M PBS, coacervates were the only structures that were observed for all Z_E/Z_R ratios tested (Figure 8a). Increasing the salt concentration to 0.3 M PBS led to the formation of coacervate−vesicle hybrid structures just as for MSG-Z_E and HCA-Z_E (Figure 8b). At 0.5 M PBS, vesicles formed with small, discrete coacervate-like structures present in the interior (Figure 8c). Since the vesicles contained dense, coacervate-like structures, they settled during DLS readings and caused sedimentation, which led to poor-quality DLS results (Figure S17). We hypothesize that the coacervate structures inside the vesicles are composed of proteins that formed intermolecular disulfide bonds with each other or the C-terminal cysteine of Z_R-ELP while in the coacervate phase.

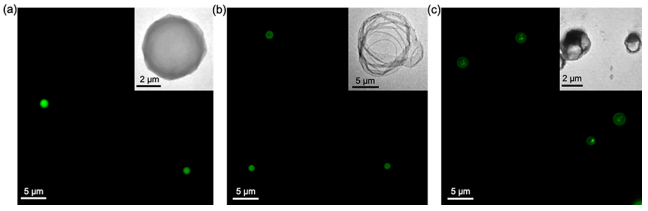

Figure 8. Confocal and TEM micrographs of phase structures that formed from mixtures of 10 μM Z_R-ELP and HGK-Z_E. (a) Coacervates observed in solutions containing 0.15 M PBS. (b) Coacervate-vesicle structure formed at 0.3 M PBS. (c) Vesicles formed at 0.10 Z_E/Z_R and 1.0 M PBS.

This disrupted the amphiphilic packing of the protein complexes. Therefore, while HGK-Z_E vesicles do follow the general coacervate to hybrid to vesicle trend with increasing salt concentrations, the unique sequence-specific nature of HGK prevents it from forming empty vesicles and clear size trends. This study showed that globular proteins in the range of 30−80 kDa should be capable of forming vesicles. However, the evaluation of the sequence and crystal structure, if available, should be performed to identify surface properties that may interfere with amphiphilic packing, including disulfide bonds or oligomerization due to hydrophobic or other interactions.[9]

Enzymatic Activity of Vesicles. One major benefit of assembling vesicles from recombinant proteins is the ability to incorporate active proteins directly into vesicles. Although active enzyme−polymer conjugate vesicles have been synthesized, they require assembly in nonpolar solvents, which can denature enzymes, and nonspecific covalent attachment of polymer to the enzyme, which decreases control over enzyme orientation and can bind active site residues, blocking access to the substrate and hindering activity.[48] To our knowledge, this is the first example of protein vesicles that are assembled from active enzymes. Because recombinant fusion of enzymes can interfere with their activity, the enzymes were genetically fused to Z_E at their exposed C-termini, based on analysis of their crystal structures, via a short GSGS linker that was used for fluorescent proteins in our previous work.[9,49] The activity was measured by UV−vis spectroscopy to demonstrate that the

https://dx.doi.org/10.1021/acs.biomac.0c00671
Biomacromolecules 2021, 22, 116−125

enzymes retained a folded structure after C-terminal fusion to Z_E and that the proteins remain functional when incorporated into vesicles (Figure 9 and Figures S18–S20).

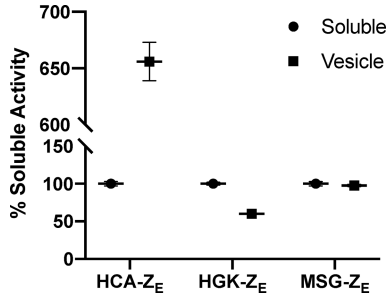

Figure 9. Relative activity of each enzyme incorporated into vesicles compared to a soluble globule-Z_E control. The activity is the average of three measurements, and the error bars represent the standard deviation.

HCA is coordinated to a Zn(II) ion that is essential for its activity and has one of the highest known enzymatic activities with a k_{cat}/K_M value of 1.5×10^8 M^{-1} s^{-1}.[25,50] Measuring the buffering activity can be difficult (equipment, complexity, and cost), so the esterase activity of HCA-Z_E was assayed instead.[32,50,51] Esters interact with the same binding pocket as bicarbonate and can serve as a surrogate to the buffering activity of HCA. HCA-Z_E exhibited a 6.5-fold activity increase upon incorporation into vesicles. One potential reason is that the substrate, 4-nitrophenyl acetate, is hydrophobic and may preferentially partition into the vesicles over the surrounding aqueous media. This would lead to an increase in the local substrate concentration and an increase in the activity. We have previously demonstrated that hydrophobic fluorescent dyes localize in the vesicles.[9,10] To demonstrate that HCA-Z_E vesicles were not disrupted upon the addition of the hydrophobic substrate, fluorescently labeled HCA-Z_E vesicles were imaged in solutions containing 1 mM 4-nitrophenyl acetate and 10 mM $ZnSO_4$ (Figure S21). It is also possible that the immobilization of the enzyme in the vesicle membrane provided a stabilizing effect.[52,53]

MSG-Z_E and HGK-Z_E have hydrophilic substrates that should not selectively partition into vesicles. Although MSG-Z_E activity was not improved upon incorporation into vesicles, it retained its activity in the presence of Mg^{2+}, glyoxylate, and acetyl CoA. The activity of HGK-Z_E, which is active in the presence of Mg^{2+} and ATP as a cofactor, decreased by ~40% when incorporated into vesicles containing coacervates. The decrease in human glucokinase activity could be due to diffusion limitations of the substrate toward the entrapped HGK-Z_E on the interior of vesicles. Additionally, some of the cysteine residues in HGK-Z_E are essential for its activity.[54] The loss of these residues due to intermolecular disulfide bond formation could disrupt the activity. These results demonstrate the potential for vesicles to be used as support materials for enzymes to aid in enzyme recovery or extend enzyme lifetime. There may be particular benefit for enzymes with hydrophobic substrates or cofactors, as the vesicles may increase the effective local concentration and improve enzyme kinetics, and this should be explored in future work.

CONCLUSION

We investigated the effects of size and charge of the globule-Z_E domain of recombinant protein vesicles to develop rational guidelines for the selection of proteins that could self-assemble into vesicles and understand how the properties of the globular proteins impact the vesicle properties. Vesicle assembly proved to be independent of the globular protein charge due to the charge screening of the high ionic strength buffers used for vesicle formation. Globule-Z_E size had a more pronounced effect on vesicle self-assembly. Increasing the globule-Z_E size tended to reduce vesicle aggregation at low Z_E/Z_R ratios and to decrease the vesicle diameter. The vesicle diameter could also be tuned, for any size protein, by increasing the ratio of Z_E/Z_R ratio and/or ionic strength. This work establishes that recombinant protein vesicles are robust with respect to both size and charge of the globular protein and can be tuned to specific applications by altering assembly conditions and the identity of the globule-Z_E domain. The significantly increased catalytic activity of HCA-Z_E, demonstrates the potential value of vesicles in biocatalysis and sensing applications. However, there may be proteins that do not readily form ideal vesicles, and it may be possible to predict these by screening for strong interglobular protein interactions. Aside from protein vesicles, this work may also offer insight into liposomes or polymersomes that are functionalized with proteins, either before or after vesicle assembly.

ASSOCIATED CONTENT

Supporting Information

The Supporting Information is available free of charge at https://pubs.acs.org/doi/10.1021/acs.biomac.0c00671.

SDS-PAGE gel analysis of sfGFP charge, turbidity profiles for stability and transition temperature measurements, epifluorescent micrographs of suprastructures, DLS intensity versus size plots, enzymatic activity assays, phase diagrams for 30 μM Z_R-ELP (PDF)

AUTHOR INFORMATION

Corresponding Author

Julie A. Champion − *School of Chemical and Biomolecular Engineering, Georgia Institute of Technology, Atlanta, Georgia 30332, United States;* orcid.org/0000-0002-0260-9392; Email: julie.champion@chbe.gatech.edu

Author

Dylan R. Dautel − *School of Chemical and Biomolecular Engineering, Georgia Institute of Technology, Atlanta, Georgia 30332, United States*

Complete contact information is available at: https://pubs.acs.org/10.1021/acs.biomac.0c00671

Author Contributions

This manuscript was written through contributions of all authors. All authors have given approval to the final version of the manuscript.

Notes

The authors declare no competing financial interest.

ACKNOWLEDGMENTS

The authors gratefully acknowledge Prof. D. Tirrell and Prof. K. Zhang for pQE60-His-Z_E/Z_R-ELP plasmid and AFIQ

Escherichia coli. This work was performed in part at the Georgia Tech Institute for Electronics and Nanotechnology, a member of the National Nanotechnology Coordinated Infrastructure, which is supported by the National Science Foundation (Grant No. ECCS-1542174). This research was financially supported by the National Science Foundation Division of Materials Research, under Award Number 1709428, and M.T. Campagna. We wish to acknowledge the core facilities at the Parker H. Petit Institute for Bioengineering and Bioscience at the Georgia Institute of Technology for the use of their shared equipment, services, and expertise.

REFERENCES

(1) Debets, M. F.; Leenders, W. P. J.; Verrijp, K.; Zonjee, M.; Meeuwissen, S. A.; Otte-Höller, I.; Van Hest, J. C. M. Nanobody-Functionalized Polymersomes for Tumor-Vessel Targeting. *Macromol. Biosci.* **2013**, *13* (7), 938−945.

(2) Dicheva, B. M.; Ten Hagen, T. L. M.; Schipper, D.; Seynhaeve, A. L. B.; Van Rhoon, G. C.; Eggermont, A. M. M.; Koning, G. A. Targeted and Heat-Triggered Doxorubicin Delivery to Tumors by Dual Targeted Cationic Thermosensitive Liposomes. *J. Controlled Release* **2014**, *195*, 37−48.

(3) Van Dongen, S. F. M.; Nallani, M.; Cornelissen, J. J. L. M.; Nolte, R. J. M.; Van Hest, J. C. M. A Three-Enzyme Cascade Reaction through Positional Assembly of Enzymes in a Polymersome Nanoreactor. *Chem. - Eur. J.* **2009**, *15* (5), 1107−1114.

(4) Gaitzsch, J.; Huang, X.; Voit, B. Engineering Functional Polymer Capsules toward Smart Nanoreactors. *Chem. Rev.* **2016**, *116*, 1053−1093.

(5) Thet, N. T.; Hong, S. H.; Marshall, S.; Laabei, M.; Toby, A.; Jenkins, A. Visible, Colorimetric Dissemination between Pathogenic Strains of Staphylococcus Aureus and Pseudomonas Aeruginosa Using Fluorescent Dye Containing Lipid Vesicles. *Biosens. Bioelectron.* **2013**, *41* (1), 538−543.

(6) Lee, K. Y.; Park, S. J.; Lee, K. A.; Kim, S. H.; Kim, H.; Meroz, Y.; Mahadevan, L.; Jung, K. H.; Ahn, T. K.; Parker, K. K.; Shin, K. Photosynthetic Artificial Organelles Sustain and Control ATP-Dependent Reactions in a Protocellular System. *Nat. Biotechnol.* **2018**, *36* (6), 530−535.

(7) Huang, X.; Li, M.; Green, D. C.; Williams, D. S.; Patil, A. J.; Mann, S. Interfacial Assembly of Protein-Polymer Nano-Conjugates into Stimulus-Responsive Biomimetic Protocells. *Nat. Commun.* **2013**, *4*, 1−9.

(8) Vargo, K. B.; Parthasarathy, R.; Hammer, D. A. Self-Assembly of Tunable Protein Suprastructures from Recombinant Oleosin. *Proc. Natl. Acad. Sci. U. S. A.* **2012**, *109* (29), 11657−11662.

(9) Park, W. M.; Champion, J. A. Thermally Triggered Self-Assembly of Folded Proteins into Vesicles. *J. Am. Chem. Soc.* **2014**, *136* (52), 17906−17909.

(10) Jang, Y.; Choi, W. T.; Heller, W. T.; Ke, Z.; Wright, E. R.; Champion, J. A. Engineering Globular Protein Vesicles through Tunable Self-Assembly of Recombinant Fusion Proteins. *Small* **2017**, *13* (36), 1700399.

(11) Egli, S.; Nussbaumer, M. G.; Balasubramanian, V.; Chami, M.; Bruns, N.; Palivan, C.; Meier, W. Biocompatible Functionalization of Polymersome Surfaces: A New Approach to Surface Immobilization and Cell Targeting Using Polymersomes. *J. Am. Chem. Soc.* **2011**, *133* (12), 4476−4483.

(12) Urry, D. W.; Long, M. M.; Cox, B. A.; Ohnishi, T.; Mitchell, L. W.; Jacobs, M. The Synthetic Polypentapeptide of Elastin Coacervates and Forms Filamentous Aggregates. *Biochim. Biophys. Acta, Protein Struct.* **1974**, *371* (2), 597−602.

(13) Urry, D. W.; Trapane, T. L.; Prasad, K. U. Phase-structure Transitions of the Elastin Polypentapeptide−Water System within the Framework of Composition−Temperature Studies. *Biopolymers* **1985**, *24* (12), 2345−2356.

(14) Jang, Y.; Hsieh, M. C.; Dautel, D.; Guo, S.; Grover, M. A.; Champion, J. A. Understanding the Coacervate-to-Vesicle Transition of Globular Fusion Proteins to Engineer Protein Vesicle Size and Membrane Heterogeneity. *Biomacromolecules* **2019**, *20* (9), 3494−3503.

(15) Moll, J. R. Designed Heterodimerizing Leucine Zippers with a Ranger of PIs and Stabilities up to 10−15 M. *Protein Sci.* **2001**, *10* (3), 649−655.

(16) Wood, C. W.; Woolfson, D. N. CCBuilder 2.0: Powerful and Accessible Coiled-Coil Modeling. *Protein Sci.* **2018**, *27* (1), 103−111.

(17) Pédelacq, J. D.; Cabantous, S.; Tran, T.; Terwilliger, T. C.; Waldo, G. S. Engineering and Characterization of a Superfolder Green Fluorescent Protein. *Nat. Biotechnol.* **2006**, *24* (1), 79−88.

(18) Hakansson, K.; Briand, C.; Zaitsev, V.; Xue, Y.; Liljas, A. Wild-Type and E106Q Mutant Carbonic Anhydrase Complexed with Acetate. *Acta Crystallogr., Sect. D: Biol. Crystallogr.* **1994**, *50* (1), 101−104.

(19) Kamata, K.; Mitsuya, M.; Nishimura, T.; Eiki, J. I.; Nagata, Y. Structural Basis for Allosteric Regulation of the Monomeric Allosteric Enzyme Human Glucokinase. *Structure* **2004**, *12* (3), 429−438.

(20) Anstrom, D. M.; Kallio, K.; Remington, S. J. Structure of the Escherichia Coli Malate Synthase G:Pyruvate:Acetyl-Coenzyme A Abortive Ternary Complex at 1.95 Å Resolution. *Protein Sci.* **2003**, *12* (9), 1822−1832.

(21) Schrödinger LLC. *PyMOL Molecular Graphics System*, Version 2.3; Schrödinger LLC, 2020.

(22) Israelachvili, J. N. *Intermolecular and Surface Forces*, 3rd ed.; Academic Press, Inc., New York, NY, 2011..

(23) Warren, N. J.; Armes, S. P. Polymerization-Induced Self-Assembly of Block Copolymer Nano-Objects via RAFT Aqueous Dispersion Polymerization. *J. Am. Chem. Soc.* **2014**, *136*, 10174−10185.

(24) Tanford, C. Thermodynamics of Micelle Formation: Prediction of Micelle Size and Size Distribution. *Proc. Natl. Acad. Sci. U. S. A.* **1974**, *71* (5), 1811−1815.

(25) Sureka, H. V.; Obermeyer, A. C.; Flores, R. J.; Olsen, B. D. Catalytic Biosensors from Complex Coacervate Core Micelle (C3M) Thin Films. *ACS Appl. Mater. Interfaces* **2019**, *11* (35), 32354−32365.

(26) Lawrence, M. S.; Phillips, K. J.; Liu, D. R. Supercharging Proteins Can Impart Unusual Resilience. *J. Am. Chem. Soc.* **2007**, *129* (33), 10110−10112.

(27) Discher, B. M.; Won, Y. Y.; Ege, D. S.; Lee, J. C. M.; Bates, F. S.; Discher, D. E.; Hammer, D. A. Polymersomes: Tough Vesicles Made from Diblock Copolymers. *Science (Washington, DC, U. S.)* **1999**, *284* (5417), 1143−1146.

(28) Lange, A. J.; Xu, L. Z.; Van Poelwijk, F.; Lin, K.; Granner, D. K.; Pilkis, S. J. Expression and Site-Directed Mutagenesis of Hepatic Glucokinase. *Biochem. J.* **1991**, *277* (1), 159−163.

(29) Chien, C. T.; Tauler, A.; Lange, A. J.; Chan, K.; Printz, R. L.; El-Maghrabi, M. R.; Granner, D. K.; Pilkis, S. J. Expression of Rat Hepatic Glucokinase in Escherichia Coli. *Biochem. Biophys. Res. Commun.* **1989**, *165* (2), 817−825.

(30) Yoshikawa, E.; Fournier, M. J.; Mason, T. L.; Tirrell, D. A. Genetically Engineered Fluoropolymers. Synthesis of Repetitive Polypeptides Containing p-Fluorophenylalanine Residues. *Macromolecules* **1994**, *27* (19), 5471−5475.

(31) Bhattacharjee, S. DLS and Zeta Potential - What They Are and What They Are Not? *J. Controlled Release* **2016**, *235*, 337−351.

(32) Verpoorte, J. A.; Mehta, S.; Edsall, J. T. Esterase Activities of Human Carbonic Anhydrases B and C. *J. Biol. Chem.* **1967**, *242* (18), 4221−4229.

(33) Requiao, R. D.; Fernandes, L.; de Souza, H. J. A.; Rossetto, S.; Domitrovic, T.; Palhano, F. L. Protein Charge Distribution in Proteomes and Its Impact on Translation. *PLoS Comput. Biol.* **2017**, *13* (5), e1005549.

(34) Der, B. S.; Kluwe, C.; Miklos, A. E.; Jacak, R.; Lyskov, S.; Gray, J. J.; Georgiou, G.; Ellington, A. D.; Kuhlman, B. Alternative Computational Protocols for Supercharging Protein Surfaces for Reversible Unfolding and Retention of Stability. *PLoS One* **2013**, *8* (5), e64363.

https://dx.doi.org/10.1021/acs.biomac.0c00671
Biomacromolecules 2021, 22, 116−125

(35) MacKay, J. A.; Callahan, D. J.; FitzGerald, K. N.; Chilkoti, A. Quantitative Model of the Phase Behavior of Recombinant PH-Responsive Elastin-like Polypeptides. *Biomacromolecules* **2010**, *11* (11), 2873−2879.
(36) Cho, Y.; Zhang, Y.; Christensen, T.; Sagle, L. B.; Chilkoti, A.; Cremer, P. S. Effects of Hofmeister Anions on the Phase Transition Temperature of Elastin-like Polypeptides. *J. Phys. Chem. B* **2008**, *112* (44), 13765−13771.
(37) Reguera, J.; Urry, D. W.; Parker, T. M.; McPherson, D. T.; Rodríguez-Cabello, J. C. Effect of NaCl on the Exothermic and Endothermic Components of the Inverse Temperature Transition of a Model Elastin-like Polymer. *Biomacromolecules* **2007**, *8* (2), 354−358.
(38) Rodríguez-Cabello, J. C.; Reguera, J.; Alonso, M.; Parker, T. M.; McPherson, D. T.; Urry, D. W. Endothermic and Exothermic Components of an Inverse Temperature Transition for Hydrophobic Association by TMDSC. *Chem. Phys. Lett.* **2004**, *388* (1−3), 127−131.
(39) Claessens, M. M. A. E.; Leermakers, F. A. M.; Hoekstra, F. A.; Cohen Stuart, M. A. Opposing Effects of Cation Binding and Hydration on the Bending Rigidity of Anionic Lipid Bilayers. *J. Phys. Chem. B* **2007**, *111* (25), 7127−7132.
(40) Tanford, C. Theory of Micelle Formation in Aqueous Solutions. *J. Phys. Chem.* **1974**, *78* (24), 2469−2479.
(41) He, C.; Hu, Y.; Yin, L.; Tang, C.; Yin, C. Effects of Particle Size and Surface Charge on Cellular Uptake and Biodistribution of Polymeric Nanoparticles. *Biomaterials* **2010**, *31* (13), 3657−3666.
(42) Feller, B. E.; Kellis, J. T.; Cascão-Pereira, L. G.; Robertson, C. R.; Frank, C. W. Interfacial Biocatalysis on Charged and Immobilized Substrates: The Roles of Enzyme and Substrate Surface Charge. *Langmuir* **2011**, *27* (1), 250−263.
(43) Alvizo, O.; Nguyen, L. J.; Savile, C. K.; Bresson, J. A.; Lakhapatri, S. L.; Solis, E. O. P.; Fox, R. J.; Broering, J. M.; Benoit, M. R.; Zimmerman, S. A.; Novick, S. J.; Liang, J.; Lalonde, J. J. Directed Evolution of an Ultrastable Carbonic Anhydrase for Highly Efficient Carbon Capture from Flue Gas. *Proc. Natl. Acad. Sci. U. S. A.* **2014**, *111* (46), 16436−16441.
(44) Meyer, D. E.; Chilkoti, A. Quantification of the Effects of Chain Length and Concentration on the Thermal Behavior of Elastin-like Polypeptides. *Biomacromolecules* **2004**, *5* (3), 846−851.
(45) Nagarajan, R. Molecular Packing Parameter and Surfactant Self-Assembly: The Neglected Role of the Surfactant Tail. *Langmuir* **2002**, *18* (1), 31−38.
(46) Meirovitch, H.; Rackovsky, S.; Scheraga, H. A. Empirical Studies of Hydrophobicity. 1. Effect of Protein Size on the Hydrophobic Behavior of Amino Acids. *Macromolecules* **1980**, *13* (6), 1398−1405.
(47) Discher, D. E.; Eisenberg, A. Polymer Vesicles. *Science* **2002**, *297*, 967−973.
(48) Huang, X.; Li, M.; Mann, S. Membrane-Mediated Cascade Reactions by Enzyme-Polymer Proteinosomes. *Chem. Commun.* **2014**, *50* (47), 6278−6280.
(49) Caparco, A. A.; Bommarius, A. S.; Champion, J. A. Effect of Peptide Linker Length and Composition on Immobilization and Catalysis of Leucine Zipper-Enzyme Fusion Proteins. *AIChE J.* **2018**, *64* (8), 2934−2946.
(50) Wilbur, K. M.; Anderson, N. G. Electrometric and Colorimetric Determination of Carbonic Anhydrase. *J. Biol. Chem.* **1948**, *176* (1), 147−154.
(51) Uda, N. R.; Seibert, V.; Stenner-Liewen, F.; Müller, P.; Herzig, P.; Gondi, G.; Zeidler, R.; Van Dijk, M.; Zippelius, A.; Renner, C. Esterase Activity of Carbonic Anhydrases Serves as Surrogate for Selecting Antibodies Blocking Hydratase Activity. *J. Enzyme Inhib. Med. Chem.* **2015**, *30* (6), 955−960.
(52) Manoel, E. A.; dos Santos, J. C. S.; Freire, D. M. G.; Rueda, N.; Fernandez-Lafuente, R. Immobilization of Lipases on Hydrophobic Supports Involves the Open Form of the Enzyme. *Enzyme Microb. Technol.* **2015**, *71*, 53−57.
(53) Bommarius, A. S. Biocatalysis: A Status Report. *Annu. Rev. Chem. Biomol. Eng.* **2015**, *6* (1), 319−345.
(54) Tiedge, M.; Richter, T.; Lenzen, S. Importance of Cysteine Residues for the Stability and Catalytic Activity of Human Pancreatic Beta Cell Glucokinase. *Arch. Biochem. Biophys.* **2000**, *375* (2), 251−260.

https://dx.doi.org/10.1021/acs.biomac.0c00671
Biomacromolecules 2021, 22, 116−125